Microchim Acta
DOI 10.1007/s00604-014-1263-0

ORIGINAL PAPER

Terahertz split-ring metamaterials as transducers for chemical sensors based on conducting polymers: a feasibility study with sensing of acidic and basic gases using polyaniline chemosensitive layer

Christoph Drexler · Tatiana V. Shishkanova · Christoph Lange · Sergey N. Danilov · Dieter Weiss · Sergey D. Ganichev · Vladimir M. Mirsky

Received: 31 January 2014 / Accepted: 14 April 2014

Abstract We report on the first application of terahertz metamaterials acting as transducers for chemical sensors based on conducting polymers. In our feasibility study aimed at sensing of gaseous hydrochloric and ammonia, a two-dimensional sensor metamaterial consisting of an array of split-ring resonators on the surface of undoped silicon wafer was prepared. The surface of the resonator was coated with a 150-μm layer of polyaniline. Binding of hydrogen chloride to polyaniline leads to distinct changes in the resonance frequency of the metamaterial. Measurements can be performed both in the reflection and transmission mode. A numerical simulation of the response revealed an increase of both the real and the imaginary components of the dielectric function of the polyaniline film. These changes are attributed to the transition from emaraldine base to emeraldine salt. The results demonstrate a new approach for formation of highly sensitive transducers for chemical sensors.

Keywords Metamaterial · Split-ring resonator · Chemical sensor · Transducer · Conducting polymer · Dielectric permittivity

C. Drexler · C. Lange · S. N. Danilov · D. Weiss · S. D. Ganichev · V. M. Mirsky
Terahertz Center, University of Regensburg, 93040 Regensburg, Germany

T. V. Shishkanova · V. M. Mirsky (✉)
Nanobiotechnology, Faculty of Natural Sciences, Brandenburg University of Technology, 01968 Senftenberg, Germany
e-mail: mirsky@b-tu.de

T. V. Shishkanova
Institute of Chemical Technology, 16628 Prague 6, Czech Republic

Introduction

During the last 20 years conducting polymers were established as a convenient and versatile material for sensing of various analytes like pH, HCl, NO_2, O_3, SO_2, inorganic ions or volatile organic compounds, for reviews see e.g. [1–6]. Such polymers have some intrinsic receptor properties toward different analytes, like for example redox active or acidic/basic compounds. Oxidation/reduction and for some polymers also protonation/deprotonation remove charge carriers in the conjugated backbone, whereas conformational changes alter planarity of the conjugated backbone leading to some restriction in the mobility of charge carriers and corresponding decrease of conductivity of this material. Chemical selectivity of conducting polymers can be modified by introducing additional receptor groups, by using molecularly imprinted polymerization of this material [2] or by formation of composites of conducting polymers with different types of nanomaterials [7–10].

A detection of analyte binding to conducting polymers can be performed by different techniques, encompassing various transducing mechanisms and frequency ranges. They comprise quartz microbalance [11], fluorescence measurements [12], UV–vis—spectroscopy [13], surface plasmon resonance [14, 15] and potentiometry [16]. Recently also radio-frequency identification devices (RFID) were successfully applied for this purpose [17]. Obviously, the mostly applied transducing mechanism is based on the measurements of the polymer resistance. A number of different measurement configurations of conductometric chemosensors with conducting polymers were suggested [18]. In the simplest sensors, two interdigitated electrodes are used. A number of more sophisticated measurement configurations, such as four-electrode chemoresistors and electrochemical chemotransistors with 3- or 6-electrode configuration were reported [18, 19].

Published online: 01 May 2014

Simultaneous application of 2- and 4-electrode configurations provides an internal sensor integrity control [19, 20] while a 6-electrode configuration allows one to get a fast sensor recovery [19]. Changes of physical properties of conducting polymers caused by their oxidation/reduction or protonation/deprotonation can be detected in a wide frequency range, starting from zero frequency (measurements of conductivity changes in DC mode), through Hz-kHz (electrochemical impedance spectroscopy) and MHz- (RFID) ranges up to the near infrared (FTIR or Raman spectroscopy [21]), and visible regime (colorimetric technique [13, 22] or surface plasmon resonance [14, 15]). Terahertz frequency range has not yet been exploited for such applications so far. However, this frequency range provides a unique advantage: it allows using metamaterials working as microscopic antenna for detection of local changes of physical properties of closely placed chemosensitive materials. Large chemosensitivity of polymers at THz/infrared frequencies and availability of straightforward and scalable fabrication methods for metamaterials, make this approach highly attractive.

We report here a new type of transducer for chemical sensors which is based on planar arrays of split-ring resonators (SRRs) embedded in conducting polymers. SRRs belong to the mostly studied types of terahertz metamaterials [23, 24] and are usually investigated in vacuum or in air. We show that due to the strong spatial confinement of the resonator mode, small changes of electrical or optical properties of the material in the gap region (conductivity, dielectric permittivity) lead to large changes of the resonance frequency. These changes of physical properties are caused by adsorption of some compounds. Deposition of receptor layers which provide selective binding of defined analytes makes this effect chemically selective. In the current work polyaniline (PANI) synthesized directly on the surface of SRRs was used as a pH-sensitive layer. The measurements were performed in THz range of frequencies corresponding to the wavelength range in vacuum 100–250 μm. Numerical simulation of the sensor response revealed an increase of both real and imaginary components of the dielectric function of the polyaniline film. The approach can be used in remote sensors based on conducting polymers.

Materials and methods

The SRR array with dimensions indicated in Fig. 1(a) was formed from gold by photolithography on undoped 0.6 mm thick silicon (Si) -wafer. The wafer was coated by a 10 nm titan (Ti) sublayer followed by a 100 nm thick gold (Au) layer. Photolithography was performed to fabricate the SRRs. The shape and dimensions of the resonators are shown in Fig. 1(a). Each resonator consists of an inductive loop and a capacitive gap, which define the *LC* resonance characteristics for light polarized along the *x*-axis [25]. In this case, the incident electric field $\boldsymbol{E}_{\text{in}} \parallel x$ drives a current through the structure which, on resonance, leads to charge accumulation at the capacitive gap and hence strong local near fields, and reduced far-field transmission. For $\boldsymbol{E}_{\text{in}} \parallel y$, the capacity of the gap does not play a role due to symmetry, resulting in a significantly higher resonance frequency since the structure responds mostly like a *dipolar* antenna [26]. The spacing between two resonators was chosen to be 3 μm in order to avoid cross-talk. The macroscopic size of the array of SRR is $10 \times 10\ \text{mm}^2$. The wafer with the resonators was treated by oxygen plasma and coated by PANI. The coating conditions were selected according to the data reviewed in [27]. By that 250 μL of 0.3 M solution of aniline in 0.5 M sulfuric acid and 250 μL of 0.27 M aqueous solution of ammonium peroxydisulfate were cooled to 0 °C, mixed and deposited onto the surface of the cooled wafer. The reaction was performed for 2 h at 0 °C. After polymerization, the formed PANI film was washed with distilled water, treated with 25 % ammonium hydroxide and dried. This leads to the conversion of the PANI film into the low conducting form of emeraldine base. The thickness of the polymer film was measured using a confocal optical profiler Pluneox from Sensofar and a value of 307±33 nm was obtained. All chemicals were obtained from Merck (www.merck.com).

Transmission experiments in the THz range were performed using a standard Fourier Transform Infrared (FTIR) spectrometer Vertex-80 (Bruker, www.bruker.com), covering the frequency range from around 1 to 8 THz. The orientation of the applied electric field in the *x*-*y* plane was manipulated using broadband wire grid polarizers [28, 29]. A vacuum sealed aluminum flow cell with quartz/TPX (4-methylpenten) windows [30] at both ends was used for transmission experiments. The illuminated area of SRRs was about 1 mm in diameter, therefore the number of excited resonators is estimated to be of the order of 10^5.

Results and discussion

The transmission through the SRR array was measured for both principle polarizations (cf. Fig. 1(b)). For $\boldsymbol{E}_{\text{in}} \parallel x$, the black line in Fig. 1(c) clearly shows a pronounced, narrow transmission minimum at 2.03 THz, which corresponds to the fundamental *LC* resonance. At around 6 THz, a more broadband feature which originates from a higher mode is observed. For $\boldsymbol{E}_{\text{in}} \parallel y$, the *dipolar* resonance leads to a minimum at around 5 THz. In the following, we will focus our discussion on the fundamental *LC* resonance at 2.03 THz which is most suitable to our purpose due to its narrow width and large local field enhancement, as detailed later. The measured spectra are superimposed by high-frequency oscillations caused by multiple interferences in the substrate. The periodicity of these oscillations fits to the thickness of the Si- substrate. The curves

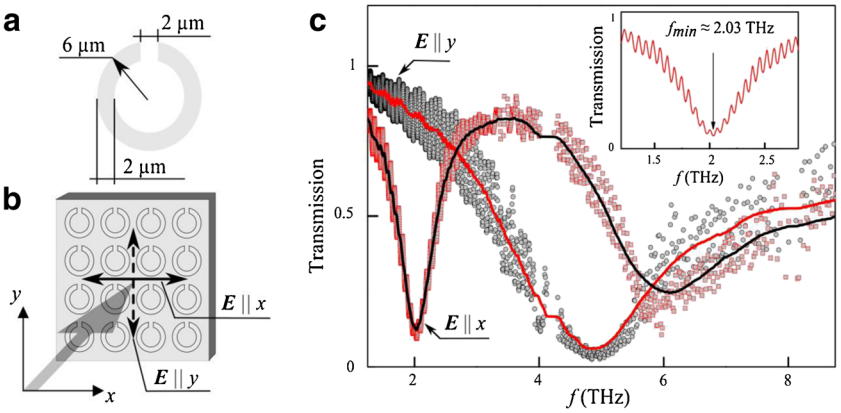

Fig. 1 **a** Design and dimensions of the split-ring resonators. **b** Experimental geometry: SRRs are oriented in the *x*-*y*-plane. The spacing between the centers of two neighboured rings in both *x*- and *y*-direction is 15 µm. *Dashed* and *full lined arrows* indicate orientations of the radiation's polarization in parallel to *x*- and *y*-direction. Transmission was measured for the resonators array illuminated at normal incidence, i.e. for the radiation electric field oriented in plane of the split-ring resonators. **c** Transmission spectra for two perpendicular polarizations: dots and squares are measured results, full lines are smoothed curves; Inset shows *LC* resonance at 2.03 THz

were smoothed by averaging over 100 neighbored points, i.e. over the spectral bandwith of 0.1 THz.

Depending on its oxidation and protonation, polyaniline can have different chemical states [31]. Polyaniline deposited by chemical polymerization has the low-conducting form of emeraldine base [27]. A deposition of this layer on the SRR array does not lead to any visible changes of the transmission spectrum of this array. However, an incubation of the sample with gaseous hydrogen chloride results in well distinguished red shift of the resonance, see Fig. 2(a). While the center frequency of the resonance shifts to around 1.8 THz, the total transmission increases by about 50 %. Subsequent treatment of these probes with ammonia (vapor over a 25 % aqueous solution) results to the blue shift of the adsorption band. The extent of the sensor regeneration depends on the incubation time (left panel in Fig. 3). The same effect is observed after heating of these probes till 150 °C for 15–30 min, see right panel in Fig. 3. An incubation of the sensor in aqueous solutions of different pH (a droplet of unbuffered HCl solutions was deposited on the sensor) leads to the pH-dependent shift of the adsorption spectrum (Fig. 4). This demonstrates that the value of the resonance shift can be used for quantitative measurements. However, a downscaling of the SRR geometry, which shifts the absorption band into near infrared range, would be very favorable for in-line applications of this sensor in aqueous environment.

We calculate the transmission characteristics of our resonators using a finite-difference frequency-domain (FDFD)

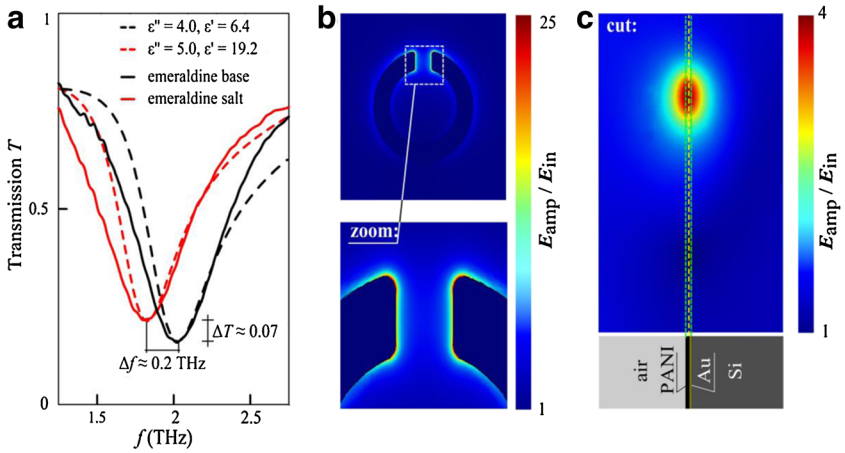

Fig. 2 **a** Black curves—transmission spectra of an array of split-ring resonators coated by polyaniline in the form of *low conducting* emeraldine base. Red curves—transmission spectra measured in the presence of HCl. The spectrum is red-shifted due to the interaction with gaseous hydrogen chloride resulting in conversion of emeraldine base into the *highly conducting* emeraldine salt. Solid lines shows measured spectra, dashed lines correspond to the results of computer simulation. The fitting parameters are ε=6.4+2.0i for the black curve and ε=19.2+5.0i for the red curve showing polymerized structure in contact with HCl. **b**–**c** Color maps of the electric field distribution under resonance condition. Plotted is the ratio between the amplified electric field, $\boldsymbol{E}_{amp}$, divided by the incoming field, $\boldsymbol{E}_{in}$. **b** Zoom into the gap region of the SRRs. **c** Cut through the layer profile

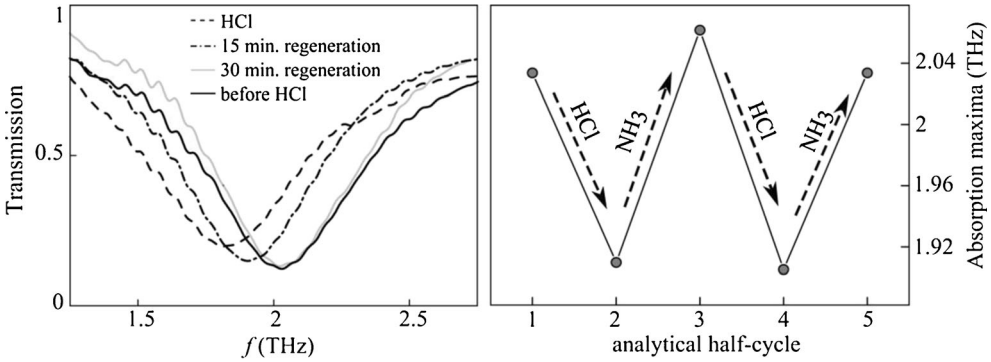

Fig. 3 Sensor regeneration by temperature and by chemical treatment. Left panel shows time-dependent recovery of the samples due to heating: The resonance shifts almost back to its starting position shown by the dashed line. Right panel depicts recovery of the transmission spectrum of the sensor contacted with 240 ppm gaseous hydrogen chloride by treatment with ammonia: The resonance shows well reproducible behavior for several analytical half-cycles

approach. The calculation yields the full near-field distribution of the resonators as a function of their dielectric environment. We use $\varepsilon_{Si}=12.6$ for the silicon substrate. For gold, a range of values for the dielectric permittivity are documented in literature, often found to depend on the crystalline state and the deposition method. However, since $\varepsilon_{Au} >> \varepsilon_{Si}$ at THz frequencies [32], the results depend only very weakly on the precise value of ε_{Au}. Hence, we approximate $\varepsilon_{Au}=\varepsilon'_{Au}+i\,\varepsilon''_{Au}\approx -10^5+10^5 i$ [32]. With the given geometry of our structures, we vary the dielectric permittivity of the PANI layer, ε_{PANI}, to match the experimentally obtained transmission spectra, as shown in Fig. 2(a). Note that for the values which the complex dielectric permittivity $\varepsilon_{PANI}=\varepsilon_{PANI}'+i\varepsilon_{PANI}''$ assumes for our experiment, the resonance frequency of the structure is predominantly dependent on ε_{PANI}', while the width of the transmission feature depends mostly on ε_{PANI}''. We obtain $\varepsilon_{PANI,base}=6.4+4i$ for emeraldine base and $\varepsilon_{PANI,salt}=19+5i$ for emeraldine salt. The observed increase of ε_{PANI}', which is caused by the conversion from emeraldine base into emeraldine salt correlates with an increase of the polymer molecular weight and polymer density [27].

In Fig. 2(b, c), the near-field distribution of the THz mode at 2.03 THz is plotted along with the geometry of our structure. Figure 2c shows the large enhancement factors $\boldsymbol{E}_{amp}/\boldsymbol{E}_{in}$ of the near field of the resonator $\boldsymbol{E}_{amp}$ relative to the incident field $\boldsymbol{E}_{amp}$. These strong near fields which prevail in the gap region of the structure demonstrate the high spatial confinement of the resonator mode, yielding a mode volume of only a few μm^3. Note that it is this volume in which the resonance frequency of the structure is most sensitive to changes of the dielectric permittivity. Although the PANI layer thickness of our structure, 300 nm, is only approximately a tenth of the near-field extension in the direction perpendicular to the surface, the well-pronounced shift of the resonance as discussed above was observed. Calculations for a 3 μm thick PANI layer with larger spatial overlap with the resonator mode (not shown) lead us to expect a 5 times larger spectral shift for the same change in dielectric properties. This aspect suggests a straight-forward pathway towards maximizing the signal-to-noise ratio and downscaling the required volume of analyte via tailoring the PANI volume to fit the mode volume of the resonator. Ultimately, this may lead to structures with μm^3-sized microreactor cells residing in the gap of a single resonator, requiring only nanoliters of analyte volume. As an important result, the simulation verifies that the fundamental mode of the SRR is highly spatially confined to the gap region, i.e., to a volume on a scale of only 10^{-3} of the corresponding vacuum wavelength, which leads to the large sensitivity of the resonance frequency of the structure to changes of the dielectric function in its gap region.

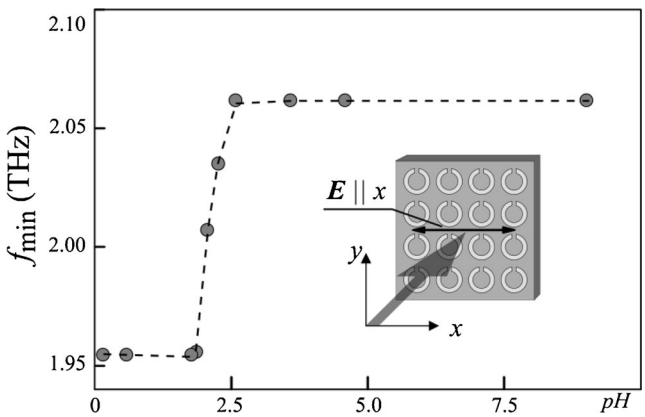

Fig. 4 pH-dependence of the red-shift of the transmission minimum

The obtained values of dielectric permittivity and their changes due to interaction with acidic compounds are very close to that reported for interaction of gaseous hydrogen chloride with poly-N-methyl-aniline at 650 nm: $\varepsilon_{base}=4.34+1.09i$ and $\varepsilon_{salt}=10.1+2.05i$ [14]. A decrease of frequency should lead to some higher values. The value of real part of dielectric permittivity at the used measurement frequency (2 THz) for a composite of polyurethane and undoped polyaniline is ~2.2; a 5 % acidic doping increases this value till ~6 [33]. It is logical to expect that pure polyaniline has a higher value of dielectric permittivity which is further

increased with increasing of doping extent. Therefore, the value of dielectric permittivity obtained from computer simulation of experimental data and its change due to interaction with acidic compounds, are close to the available literature data. The strong effect of this change on the resonance frequency of the array of split ring resonators provides a possibility to use this type of metamaterials as a new transducer to detect such interaction.

Chemosensitive properties of polyaniline which we used in this work as chemosensitive material are well known. Its selectivity towards particular analytes can be optimized or adjusted using chemical modification [1–3, 13, 34–38]. Instead of polyaniline other types of chemosensitive materials can be used [1–6].

In this work we have performed spectral measurements which allowed us to make a complete characterization of the transducer and recalculation of changes of optical parameters of chemosensitive layer. For particular applications in chemical sensing, measurements at single wavelength using a laser or other monochromatic light source can be performed. Scaling of metamaterial provides a technological possibility to adjust the adsorption spectrum of the sensor to the irradiation wavelength of suitable lasers. The value of the intensity change in the current work was about 50 % at 2.03 THz for 240 ppm of HCl. Assuming typical values of dynamic range for the measurements of light intensity as ~10^4–10^5, we can estimate the instrumental value of the limit of detection of detection of this sensor as tens of ppb which is about the same as for conductometric sensors. Further improvement of sensitivity can be reached by optimization of the design of metamaterials with the goal to get a narrow resonance peak [39], such works are now in progress.

Conclusion

The lack of simple and inexpensive instrumentation for terahertz range resulted to the ignoring of possibilities of this range in the development of technologies of chemical sensing. The situation was changed during last years—an intensive development of irradiation sources and measurement techniques made this range also perspective for different applications. In the case of analytical applications, this provided a possibility to exploit a novel class of transducers for chemical sensors—metamaterials. Here we have demonstrated a new transducing mechanism based on planar array of SRRs. One can expect that a further implementation of this allows one to combine advantages of optical measurement techniques, such as remote sensing and parallelized reading of sensor arrays, with high sensitivity and dynamic range of electrical measurement techniques.

To summarize, we have demonstrated that split-ring metamaterials based on conducting polymers can be applied as transducer elements in chemical sensing. Since the fundamental mode of the SRR is highly spatially confined to the micron-sized gap region enables local or even spatially resolved studies of chemicals, or, more courageously, downscaling devices to single-resonator structures with fluidic microchannels which may ultimately enable processing nanoliter-scale analyte volumes. While our measurements are carried out on simple spit-ring resonators excited at terahertz frequencies a large variety of easily scalable designs of state-of-the-art metamaterials with lower line widths and mode volumes would allow developing sensors with substantially higher physical sensitivity and a wide range of frequencies.

Acknowledgments The authors are grateful to C. Linz for preparing the SRR arrays, Prof. R. Huber, Prof. M. Koch and Dr. C. Jansen for fruitful discussions, Dr. U. Lange for participating in preliminary experiments and Prof. J. Acker for the measurements of polymer thickness. We thank the DFG (SFB689) and Linkage Grant of IB of BMBF at DLR.

References

1. McQuade DT, Pullen AE, Swager TM (2000) Conjugated polymer-based chemical sensors. Chem Rev 100:2537–2574
2. Lange U, Roznyatovskaya NV, Mirsky VM (2008) Conducting polymers in chemical sensors and arrays. Anal Chim Acta 614:1–26
3. Hua B, Shi G (2007) Gas sensors based on conducting polymers. Sensors 7:267–307
4. Trojanowicz M (2003) Application of conducting polymers in chemical analysis. Microchim Acta 143:75–91
5. Heinze J, Frontana-Uribe BA, Ludwigs S (2011) Electrochemistry of conducting polymers - persistent models and new concepts. Chem Rev 110:4724–4771
6. Inzelt G (2008) Conducting polymers. A new era in electrochemistry. Springer, Berlin
7. Tsakova V, Ivanov S, Lange U, Stoyanova A, Lyutov V, Mirsky VM (2010) Electroanalytical applications of nanocomposites from conducting polymers and metallic nanoparticles prepared by layer-by-layer deposition. Pure Appl Chem 83:345–358
8. Hatchett DW, Josowicz M (2008) Composites of intrinsically conducting polymers as sensing nanomaterials. Chem Rev 108: 746–769
9. Kochmann S, Hirsch T, Wolfbeis OS (2012) Graphenes in chemical sensors and biosensors. Trends Anal Chem 39:87–113
10. Rajesh AT, Kumar D (2009) Recent progress in the development of nano-structured conducting polymers/nanocomposites for sensor applications. Sens Actuators B 136:275–286
11. Deng Z, Stone DC, Thompson M (1997) Characterization of polymer films of pyrrole derivatives for chemical sensing by cyclic voltammetry, X-ray photoelectron spectroscopy and vapour sorption studies. Analyst 122:1129–1138
12. Thomas SW III, Joly GD, Swager TM (2007) Chemical sensors based on amplifying fluorescent conjugated polymers. Chem Rev 107:1339–1386
13. Pringsheim E, Terpetschnig E, Wolfbeis OS (1997) Optical sensing of pH using thin films of substituted polyanilines. Anal Chim Acta 357:247–252
14. Samoylov AV, Mirsky VM, Hao Q, Swart C, Shirshov YM, Wolfbeis OS (2005) Nanometer-thick SPR sensor for gaseous HCl. Sens Actuators B 106:369–372

15. Pernites R, Ponnapati R, Felipe MJ, Advincula R (2011) Electropolymerization molecularly imprinted polymer (E-MIP) SPR sensing of drug molecules: pre-polymerization complexed terthiophene and carbazole electroactive monomers. Biosens Bioelectron 26:2766–2771
16. Bobacka J, Ivaska A (2007) Ion sensors with conducting polymers as ion-to-electron transducers. In: Alegret S, Merkoci A (eds) Comprehensive analytical chemistry, vol. 49. Electrochemical sensor analysis. Elsevier, Amsterdam, pp 73–86
17. Potyrailo RA, Morris WG (2007) Multianalyte chemical identification and quantitation using a single radio frequency identification sensor. Anal Chem 79:45–51
18. Lange U, Mirsky VM (2011) Chemiresistors based on conducting polymers: a review on measurement techniques. Anal Chim Acta 687:105–113
19. Lange U, Mirsky VM (2011) Integrated electrochemical transistor as a fast recoverable gas sensor. Anal Chim Acta 687:7–11
20. Lange U, Mirsky VM (2008) Separated analysis of bulk and contact resistance of conducting polymers: comparison of simultaneous 2- and 4-point measurements with impedance measurements. J Electroanal Chem 622:246–251
21. Christie S, Scorsone E, Persaud K, Kvasnik F (2003) Remote detection of gaseous ammonia using the near infrared transmission properties of polyaniline. Sens Actuat B 90:163–169
22. Pirsa S, Alizadeh A (2012) A selective DMSO gas sensor based on nanostructured conducting polypyrrole doped with sulfonate anion. Sens Actuators B 168:303–309
23. Engheta N, Ziolkowski NW (eds) (2006) Metamaterials: physics and engineering explorations. Wiley, New York
24. Klein MW, Enkrich C, Wegener M, Soukoulis CM, Linden S (2006) Single-slit split-ring resonators at optical frequencies: limits of size scaling. Opt Lett 31:1259–1261
25. Padilla WJ, Taylor AJ, Highstrete C, Lee M, Averitt RD (2006) Dynamical electric and magnetic metamaterial response at terahertz frequencies. Phys Rev Lett 96:107401.1–107401.4
26. O'Hara J, Smirnova E, Azad AK, Chen H-T, Taylor AJ (2007) Effects of microstructure variations on macroscopic Terahertz metafilm properties. Act Passive Electron Components. doi:10.1155/2007/49691
27. Stejskal J, Gilbert RG (2002) Polyaniline. A preparation of a conducting polymer. Pure Appl Chem 74:857–867
28. Ziemann E, Ganichev SD, Yassievich IN, Perel VI, Prettl W (2000) Characterization of deep impurities in semiconductors by terahertz tunneling ionization. J Appl Phys 87:3843–3849
29. Karch J, Olbrich P, Schmalzbauer M, Zoth C, Brinsteiner C, Fehrenbacher M, Wurstbauer U, Glazov MM, Tarasenko SA, Ivchenko EL, Weiss D, Eroms J, Ganichev SD (2010) Dynamic Hall effect driven by circularly polarized light in a graphene layer. Phys Rev Lett 97:227402.1–227402.4
30. Ganichev SD, Prettl W (2006) Intense terahertz excitation of semiconductors. Univ Press, Oxford
31. Syed AA, Dinesan MK (1991) Review: polyaniline - a novel polymeric material. Talanta 38:815–837
32. Olmon RL, Slovick B, Johnson TW, Shelton D, Oh SH, Boreman GD, Raschke MB (2012) Optical dielectric function of gold. Phys Rev B86:235147–235147
33. Nguema E, Vigneras V, Miane JL, Mounaix P (2008) Dielectric properties of conducting polyaniline films by THz time-domain spectroscopy. Eur Polym J 44:124–129
34. Ando M, Swart C, Pringsheim E, Mirsky VM, Wolfbeis OS (2005) Optical ozone sensing properties of poly(2-chloroaniline), poly(N-methylaniline) and polyaniline films. Sens Actuators B 108:528–534
35. Mirsky VM, Kulikov V, Hao Q, Wolfbeis OS (2004) Multiparameter high throughput characterization of combinatorial chemical microarrays of chemosensitive polymers. Macromol Rapid Commun 2004(25):253–258
36. Piletsky SA, Panasyuk TL, Piletskaya EV, Elskaya AV, Pringsheim E, Wolfbeis OS (2000) Polyaniline-coated micro titer plates for use in longwave optical bioassays. Fresenius J Anal Chem 366:807–810
37. Haynes A, Gouma P-I (2009) Polyaniline-based environmental gas sensors. In: Baraton M-I (ed) Sensors for environment, health and security. Springer, Berlin, pp 451–459
38. Song E, Choi JW (2013) Conducting polyaniline nanowire and its applications in chemiresistive sensing. Nanomaterials 3:498–523
39. Jansen C, Al-Naib IAI, Born N, Koch M (2011) Terahertz metasurfaces with high Q-factors. Appl Phys Lett 98:051109.1–051109.3